

ABSTRACT

BACKGROUND: Development of novel immunotherapeutics in oncology is of crucial interest and their good testing at preclinical stage relies on i) the features of the animal model used and ii) the application of an appropriate comprehensive strategy for the deep delineation of mechanisms underlying resistance/sensitivity to a drug.

METHODS: Using a syngeneic sarcoma mouse model, treated with anti-PDL1, we investigated by intratumoral microdialysis and flow cytometry the immunometabolic profile and immune landscape of the tumor, respectively. The anti-tumor effect of PDL1 blockade was assessed through tumor growth monitoring and tumoral biopsies were also collected for gene expression analysis. Finally, involvement of CD8 T cells in the anti-tumor PDL1 blockade-mediated activity was addressed using a specific depleting antibody-based strategy.

RESULTS: When compared to a non-tumor area, data obtained from tumor microdialysates highlighted i) a slight Kynurenine pathway activation, ii) a strong Arginase activity, and iii) a high Adenosine production. Interestingly, anti-PDL1 effect was associated with a decrease of the tumoral Adenosine level thus arguing for an important role of the Adenosine axis in the control of the anti-tumor immune response. In addition, PDL1 blockade led to an intratumoral CD45+ leukocytes enrichment, with a higher abundance of lymphocytes also displaying increased level of IFN γ . In contrast, macrophages – CD11b+/F4:80+ - were limited upon treatment, especially the immunosuppressive CD11b/Gr1Low/Int cell subsets, in favor of an increase of the M1/M2 macrophages ratio. Interestingly, CD8 depletion fully abrogated anti-PDL1 anti-tumor effect thus showing the unequivocal role of this population. Finally, gene expression analysis revealed, in addition to an interferon signature, changes in genes from the myeloid / neutrophil subsets including Arg1 and key chemokines.

METHODS

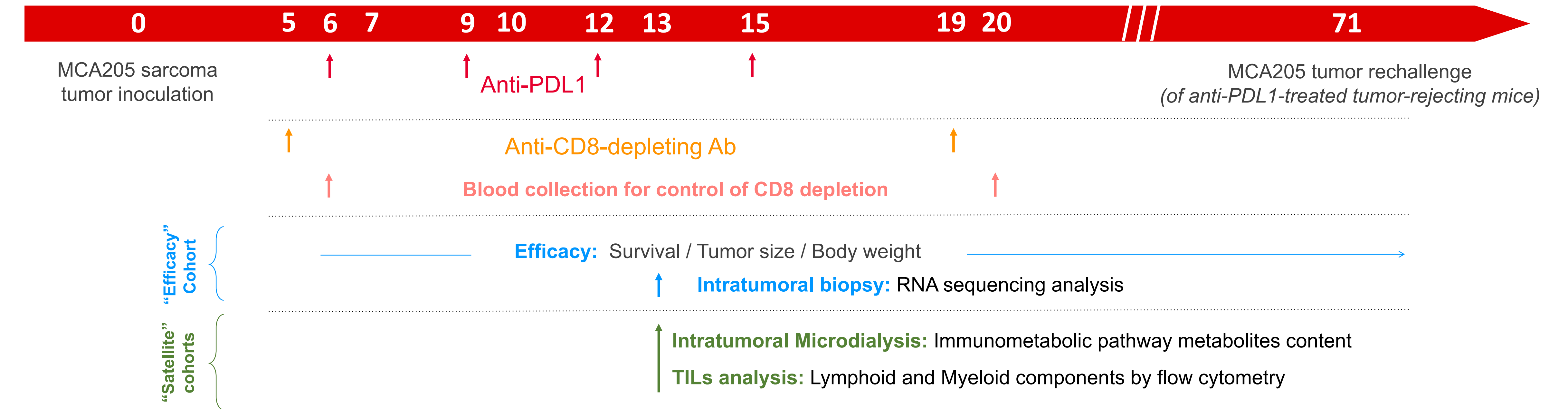


Figure 1: After MCA205 sarcoma tumor inoculation in immunocompetent C57BL/6J mice, animals were allocated to the treatment groups and processed either for "efficacy" or as "satellites", for the respective experiments and readouts as mentioned above.

RESULTS

In vivo monitoring

PDL1 blockade triggers an anti-tumor response in the MCA205 sarcoma model

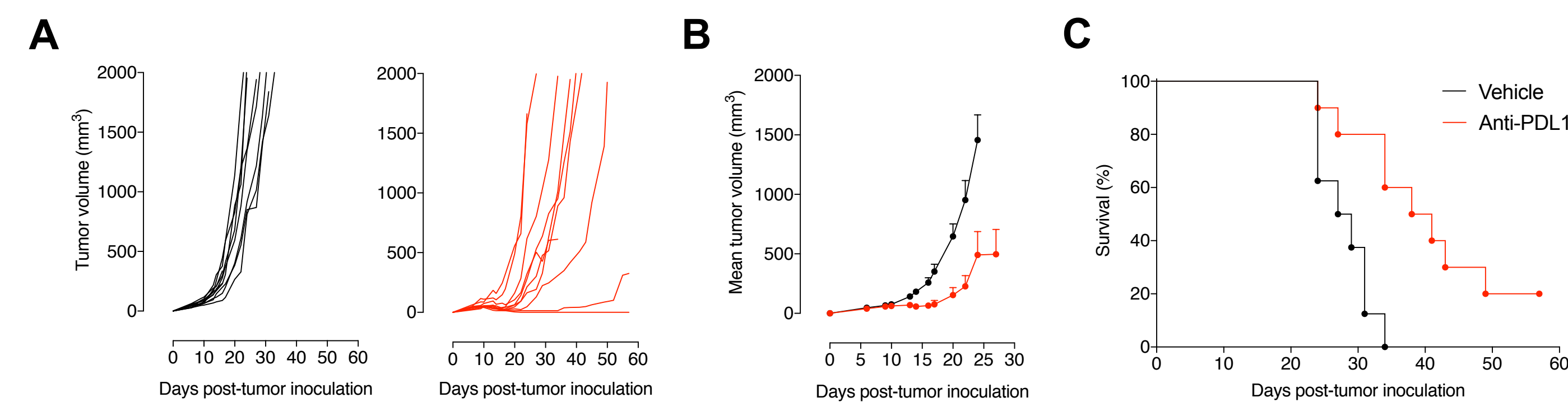


Figure 2: Individual (A) and mean (B) tumor volume (mm³), and Kaplan-Meier plot survival (C) of MCA205 tumor-bearing mice upon vehicle (n=10) and anti-PDL1 antibody (n=10) treatments.

Immunometabolic landscape

MCA205 model exhibits a suppressive immunometabolic profile involved in the MoA of anti-PDL1

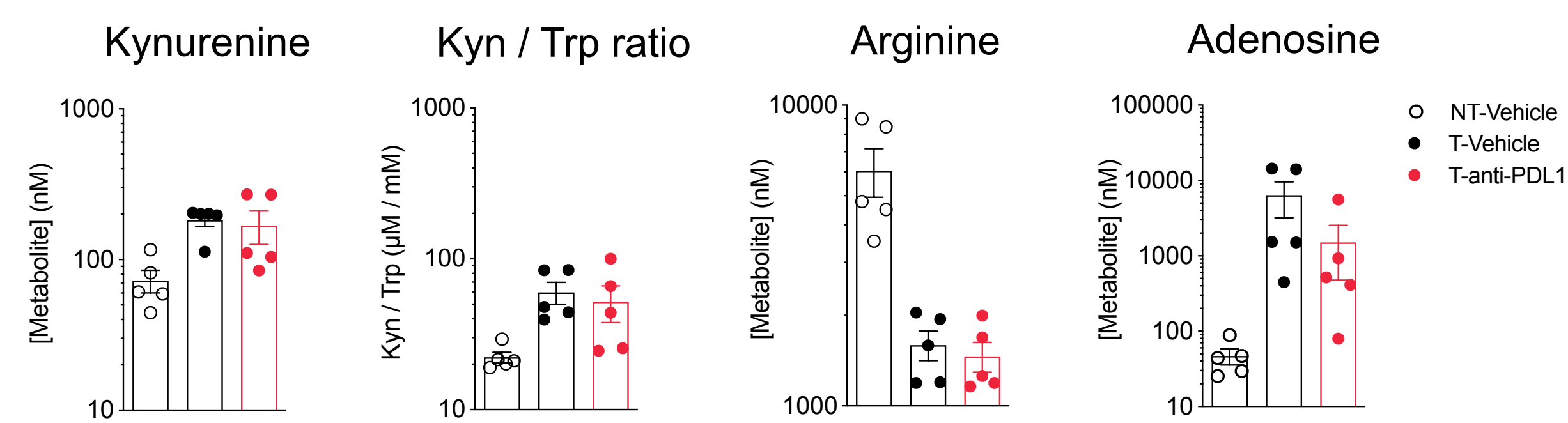


Figure 3: Immunometabolic pathways profiling of MCA205 tumors on day 13 post-tumor inoculation (200mm³ average volume) by intratumoral microdialysis and metabolite level determination by LC/MS.

RNA-sequencing analysis on intratumoral biopsies

Gene expression analysis reveals an inflammatory response driven by an interferon signaling signature

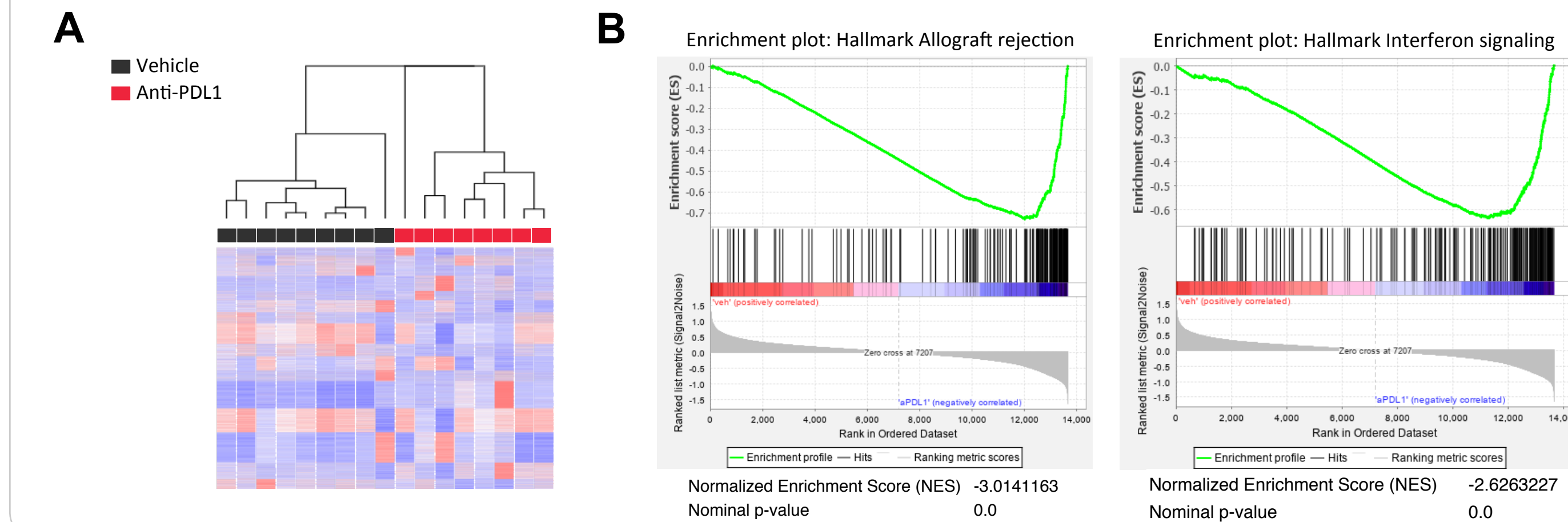


Figure 4: Intratumoral gene expression analysis by mean of RNA-sequencing (A) reveals a proper unsupervised clustering of samples and (B) highlights a strong and significant enrichment in genes belonging to Allograft rejection and Interferon signaling hallmarks datasets.

Tumor immunoprofiling

PDL1 blockade favors lymphoid immune cell MCA205 tumor infiltrate

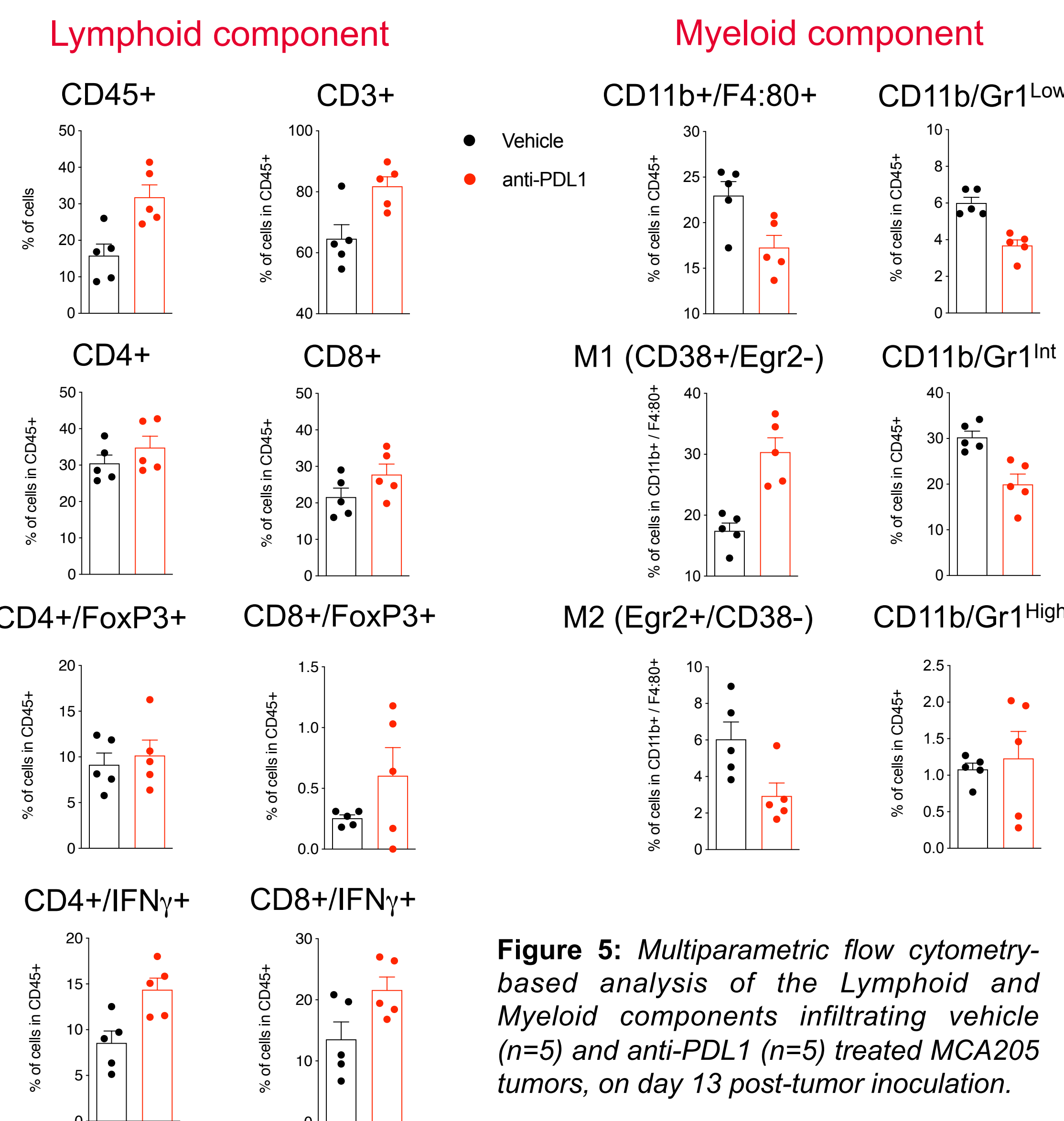


Figure 5: Multiparametric flow cytometry-based analysis of the Lymphoid and Myeloid components infiltrating vehicle (n=5) and anti-PDL1 (n=5) treated MCA205 tumors, on day 13 post-tumor inoculation.

CD8 depletion effectiveness

PDL1 blockade anti-tumor activity is CD8 T cell-driven

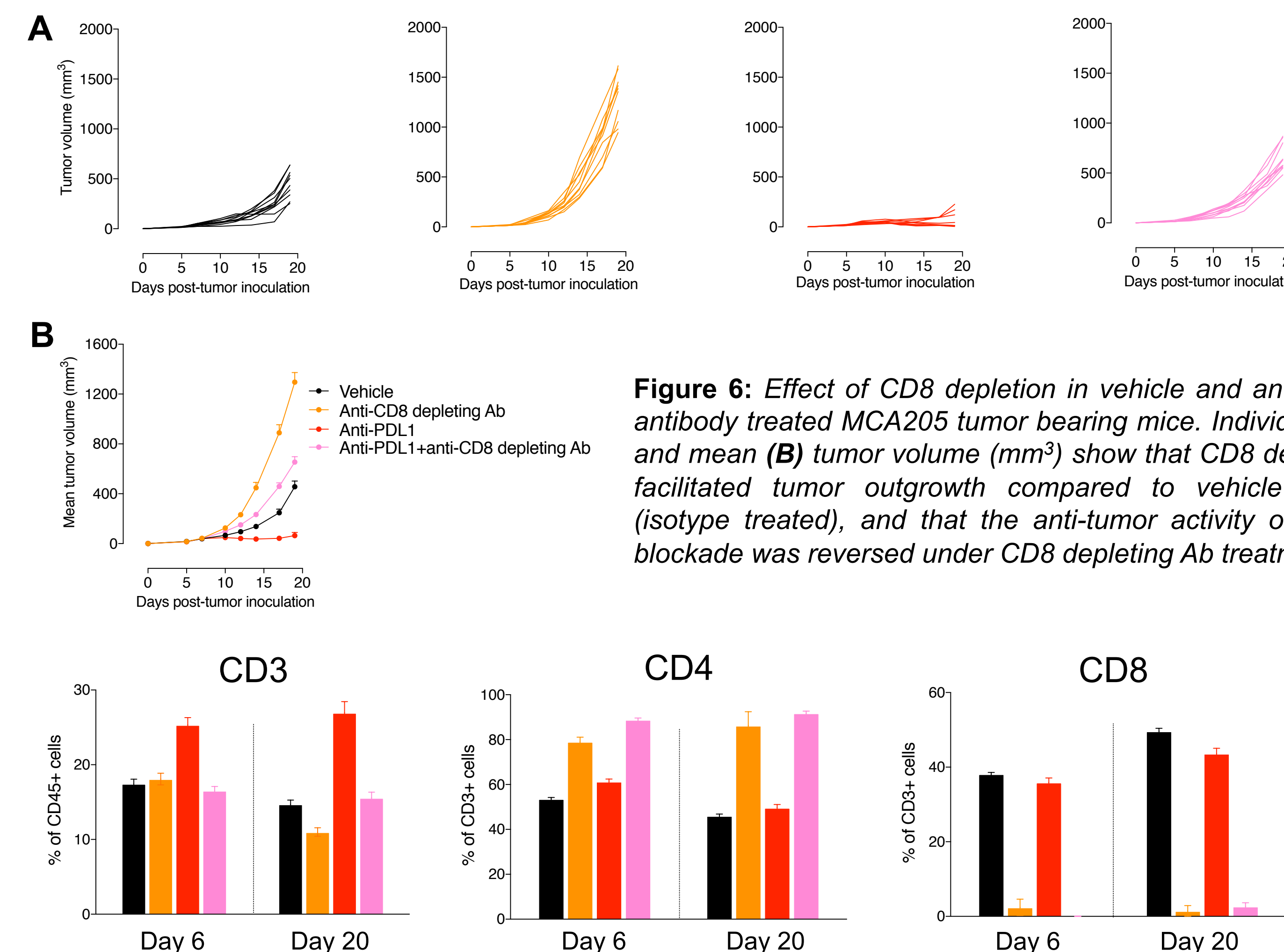


Figure 6: Effect of CD8 depletion in vehicle and anti-PDL1 antibody treated MCA205 tumor bearing mice. Individual (A) and mean (B) tumor volume (mm³) show that CD8 depletion facilitated tumor outgrowth compared to vehicle group (isotype treated), and that the anti-tumor activity of PDL1 blockade was reversed under CD8 depleting Ab treatment.

Figure 7: Blood immunoprofiling supports the effectiveness of CD8 depletion. Flow cytometry monitoring of CD3, CD4, and CD8 cells in peripheral blood samples, 1 day and 2 weeks after the 1st injection of CD8-depleting Ab. CD8-depleting Ab produced an efficient and stable CD8 depletion concomitantly with a higher proportion of CD4 T cells.

In vivo monitoring of tumor rechallenged rejecting mice

Anti-PDL1 mediated tumor rejection leads to the development of a memory immune response independent from CD8

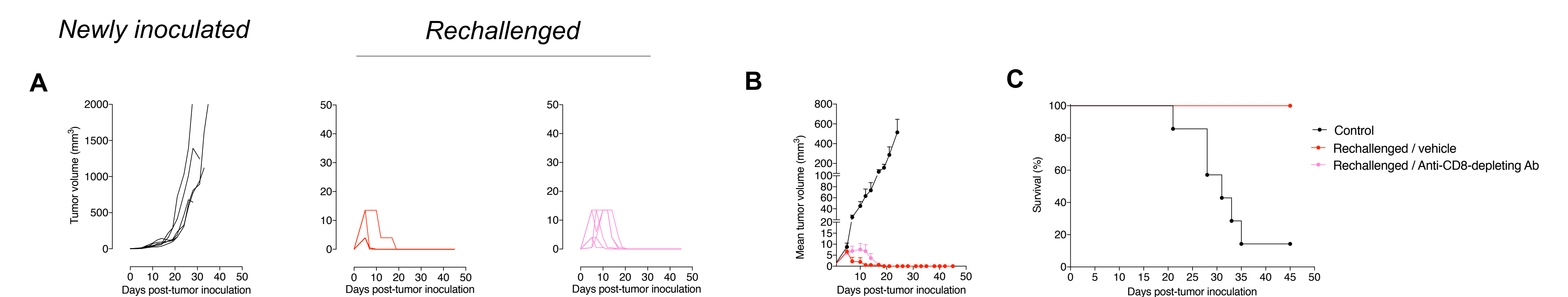


Figure 8: Anti-PDL1 antibody-mediated MCA205 tumor-rejecting mice were rechallenged with MCA205 cells on day 71 post-1st challenge, and treated or not with anti-CD8-depleting Ab. Individual (A) and mean (B) tumor volume (mm³), and Kaplan-Meier plot survival (C) show that PDL1 blockade-induced tumor rejection results in and is mediated by a memory immune response, CD8-independent.

CONCLUSIONS & PERSPECTIVES

This study on the syngeneic MCA205 sarcoma mouse model shows that this PDL1-responding model is featured of a specific suppressive immunometabolic profile, itself involved, at least partially, in the response to an anti-PDL1 antibody. Anti-tumor activity of PDL1 blockade is indeed shown to be underpinned by a great impact on the immune system, involving the development of a pro-inflammatory profile of tumor immune cell infiltrate, and CD8-driven response.

Interestingly, this multiparametric dataset evidences that while an anti-tumor immune-driven response can be evaluated through in vivo monitoring, profiling immune function in parallel by the mean of relevant models and immunological readouts permits for providing a deeper understanding of how a cancer therapy performs, and might thus serve to thoroughly explore novel immunotherapeutics.